# VLBA Scientific Memorandum 31: ASTROMETRIC CALIBRATION OF mm-VLBI USING SOURCE FREQUENCY PHASE REFERENCED OBSERVATIONS

Richard Dodson and María Rioja
International Centre for Radio Astronomy Research (ICRAR), UWA, Australia
Observatorio Astronómico Nacional, España

November 24, 2009

## ABSTRACT

In this document we layout a new method to achieve "bona fide" high precision Very Long Baseline Interferometry (VLBI) astrometric measurements of frequency-dependent positions of celestial sources (even) in the high (mm-wavelength) frequency range, where conventional phase referencing techniques fail. Our method, dubbed SOURCE/FREQUENCY PHASE REFERENCING (SFPR) combines *fast frequency switching* (or dual-frequency observations) with the *source switching* of conventional phase referencing techniques. The former is used to calibrate the dominant highly unpredictable rapid atmospheric fluctuations, which arise from variations of the water vapor content in the troposphere, and ultimately limit the application of conventional phase referencing techniques; the latter compensates the slower time scale remaining ionospheric/instrumental, non-negligible, phase variations.

For cm-VLBI, the SFPR method is equivalent to conventional phase referencing applied to the measurement of frequency-dependent source positions changes ("core-shifts"). For mm-VLBI, the SFPR method stands as the only approach which will provide astrometry. A successful demonstration of the application of this new astrometric analysis technique to the highest frequency VLBA observations, at 86 GHz, is presented here. Our previous comparative astrometric analysis of cm-VLBI observations, presented elsewhere, produced equivalent results using both methods.

In this memo we layout the scope and basis of our new method, along with a description of the strategy (Sections 1 and 2), and a demonstration of successful application to the analysis of VLBA experiment BD119 (Section 3). Finally, in Section 4, we report on the results from a series of 1-hour long VLBA experiments, BD123A, B and C, aimed at testing the robustness of the method under a range of weather conditions.


# 1 Introduction

One of the complications in VLBI, over connected array interferometers, arises from the completely unrelated atmospheric conditions that the wavefronts propagate through before reaching the widely separated antennae. Self calibration procedures, which are the standard VLBI analysis technique for imaging radio sources, rely on closure relations to remove the station dependent complex gain factors that characterize the phase errors at each antenna. A direct detection of the source with good signal to noise ratio is required within every segment of the coherence integration time-interval. This time interval is set by the stability of the instrument and, dominantly, the atmospheric turbulence. An important consequence of the use of phase closure is that information on the absolute position of the source is lost, preventing the measurement of astrometric quantities.

The application of phase-referencing techniques, to the analysis of interleaving observations of the program source and a nearby calibrator, preserves

the information on the angular separation on the sky and provides high precision relative-astrometry (Alef 1988, Beasley & Conway, 1995). At the observations, the scans on the scientifically interesting source, the target, are interleaved (within the coherence integration time) with observations of a calibrator source, the reference. The antenna-based corrections derived from the self-calibration analysis of the reference source observations are transferred for the calibration of the target source. Next, the target dataset is Fourier transformed without any further calibration to yield a phase referenced map of the target source, where the position offset of the peak from the center provides a precise measurement of the relative separation between both sources. The propagation of astrometric errors in the phase referencing analysis is strongly dependent on the angular separation between the target and reference sources, and range between the micro-arcsec and tenths of milli-arcsec accuracy. This phase referencing technique, from now on referred as "conventional phase referencing", is well established and has been used to provide high precision astrometric measurements of (relative) source positions in cm-VLBI observations.

It would be highly desirable to extend this capability to the mm-VLBI regime, yet at the highest frequencies the observations are sensitivity limited: the instruments are less efficient, the sources are intrinsically weaker, and the phase coherence integration times are severely constrained by the rapid atmospheric phase fluctuations due to the variations (spatial and temporal) of the water vapor content in the troposphere. In particular, the coherence time is too short to allow an antenna to switch its pointing direction between pairs of sources, in all but the most exceptional cases (Porcas & Rioja, 2002), within that time range. The lack of suitable reference sources in mm-VLBI makes it almost impossible to apply "conventional phase referencing" techniques in the high frequency (i.e. significantly above 43 GHz) domain.

Therefore it would be hugely beneficial if the calibration could be performed at a lower, easier, frequency and used for data collected at a higher frequency. That is, to transfer the calibration terms (for phase/delay/rate VLBI observables) derived at a different frequency rather than at a different source as in "conventional phase-referencing". It should be noted that frequency switching can be performed much faster than source switching at the VLBA. Moreover the duty-cycle is now determined by the coherence time at the lower frequency. The low frequency phases provide 'connection' but of course can not correct for variations faster than the duty cycle. This requires co-temporal dual frequency observations as provided by the next generation of VLBI antennae and arrays which are able to co-observe at different frequency bands, e.g. the Yebes 40m antenna and the Korean VLBI Network.

The feasibility of multi-frequency observations to correct the non-dispersive tropospheric phase fluctuations in the high frequency regime has been studied for some time. It relies on the fact that such fluctuations will be linearly proportional to the observing frequency, and hence it should be possible to use a scaled version of the calibration terms derived from the analysis of observations at a

lower frequency (where more and stronger sources are available, with longer coherence integration times and better antenna performance), to calibrate higher frequency observations. It is a kind of phase referencing, between observations at two frequencies, that we call "frequency phase transfer" (FPT). Among the earliest references we found are "Phase compensation experiments with the paired antennas method 2. Millimeter-wave fringe correction using centimeter-wave reference" (Asaki, et al. 1998) with the Nobeyama millimeter array (NMA), and "Tropospheric Phase Calibration in Millimeter Interferometry" (Carilli & Holdaway, 1999) for application with the Very Large Array (VLA). In "VLBI observations of weak sources using fast frequency switching", Middelberg et al. (2005) applied this frequency phase transfer technique to mm-VLBI observations. They achieved a significant increase in coherence time, resulting from the compensation of the rapid tropospheric fluctuations, but failed to recover the astrometry, due to the remaining residual dispersive terms.

Our proposed SOURCE/FREQUENCY PHASE REFERENCING method endows this approach with astrometric capability for measuring frequency dependent source positions ("core-shifts") by adding a strategy to estimate the ionospheric (and other) contributions. In "Measurement of core-shifts with astrometric multi-frequency calibration" (Rioja et al. 2005) we applied it to measure the "core-shift" of quasar 1038+528 A between S and X-bands (8.3/2.2 GHz), and validate the results by comparison with those from standard phase referencing techniques at cm-VLBI, where both methods are equivalent.
Here we present a demonstration of successful application of the SFPR method to astrometric mm-VLBI, a much more challenging frequency regime where conventional phase referencing fails. Also, the basis of the method, and details on the scheduling and data analysis are described.
This method opens a new horizon with targets and fields suitable for high precision astrometric studies with VLBI, especially at high frequencies where severe limitations imposed by the rapid fluctuations in the troposphere prevent the use of conventional phase referencing techniques. In addition this method can be applied to Space VLBI, where accurate orbit determination is a significant issue. This method results in perfect correction of frequency independent errors, such as those arising from the uncertainty in the reconstruction of the satellite orbit. The application to the space mm-VLBI mission VSOP-2 is described in detail in Rioja & Dodson (2009).

## 2 The Basis of the new astrometric method

This section outlines the basis of an astrometric method aimed at measuring the frequency dependent core position shift ("core-shift" hereafter) in radio sources in the high frequencies regime. The novel SFPR approach consists of two calibration steps:

- Dual-frequency observations to calibrate the rapid non-dispersive atmospheric phase fluctuations in VLBI observables at the high frequency

regime, arising from inhomogeneities in the water vapor content in the troposphere and

- Dual-source observations to compensate for the remaining dispersive slower varying contributions to the observed phases.

The first step results in increased coherence times at the higher frequency, however, an extra step of calibration which involves observations of a second source is needed to preserve the astrometry. This is the essence of the SFPR technique.

We include here a description of the procedure using conventional formulae for VLBI - and assume that the data reduction is done using AIPS. Dodson & Rioja (2008) contains more prescriptive details. Its application involves observations with fast frequency switching between the two frequencies of interest (*high* and *low*, shown as superscripts in the formulae, for the higher and lower observed frequencies), and slow source switching between the target and a nearby source ($A$ and $B$, shown as subscripts in the formulae). Following standard nomenclature, the residual phase (that is after a priori estimated values for the various contributing terms have been removed and the signal integrated in the correlator) values for observations of the target source ($A$) at the lower frequency (*low*) with a given baseline, $\phi_A^{low}$, are shown as a sum of contributions:

$$\phi_A^{low} = \phi_{A,geo}^{low} + \phi_{A,tro}^{low} + \phi_{A,ion}^{low} + \phi_{A,inst}^{low} + \phi_{A,str}^{low} + 2\pi n_A^{low}, \quad \text{with } n_A^{low} \text{ integer}$$

where $\phi_{A,geo}^{low}, \phi_{A,tro}^{low}, \phi_{A,ion}^{low}$ and $\phi_{A,inst}^{low}$ are, respectively, contributions to the residual phase from geometric, propagation medium – troposphere and ionosphere – and instrumental errors, and $\phi_{A,str}^{low}$ is the radio structure term (the visibility phase), referenced to the point for which $\phi_{A,geo}^{low}$ has been computed, which is non-zero for non-symmetric sources; $2\pi n$ stands for the modulo $2\pi$ phase ambiguity term.

The application of "self-calibration" techniques produces an image of the source, which allows one to disentangle the effect of the visibility phase from the rest of contributions, and produce a set of antenna-based terms, $\phi_{A,self-cal}^{low}$, that account for the errors mentioned above.

These terms are scaled by the frequency ratio $R$, after interpolation to the observing times of the higher frequency scan times observations, $\tilde{\phi}_{A,self-cal}^{low}$, and used to calibrate the higher frequency observations.

The resultant frequency-referenced residual phases at the higher frequency $\phi_A^{FPT}$ are:

$$\phi_A^{FPT} = \phi_A^{high} - R \,.\, \tilde{\phi}_{A,self-cal}^{low} =$$
$$= \phi_{A,str}^{high} + (\phi_{A,geo}^{high} - R \,.\, \tilde{\phi}_{A,geo}^{low}) + (\phi_{A,tro}^{high} - R \,.\, \tilde{\phi}_{A,tro}^{low}) + (\phi_{A,ion}^{high} - R \,.\, \tilde{\phi}_{A,ion}^{low}) +$$
$$+ (\phi_{A,inst}^{high} - R \,.\, \tilde{\phi}_{A,inst}^{low}) + 2\pi(n_A^{high} - R \,.\, n_A^{low}) \qquad (1)$$

where $FPT$ stands for "Frequency Phase Transfer" and $\tilde{\phi}$ stands for the interpolated *low*-frequency self-calibration solutions to the *high*-frequency scan times. This calibration strategy results in perfect cancellation (as long as the interpolation of $\tilde{\phi}$ is a good approximation to $\phi$) of the non-dispersive rapid tropospheric phase fluctuation terms, since:

$$\phi^{high}_{A,tro} - R\,.\,\tilde{\phi}^{low}_{A,tro} = 0$$

but not for the dispersive ones, which do not scale linearly with frequency, and hence there are remaining ionospheric and instrumental terms:

$$\phi^{high}_{A,ion} - R\,.\,\tilde{\phi}^{low}_{A,ion} = (\tfrac{1}{R} - R)\,\tilde{\phi}^{low}_{A,ion}$$
$$\phi^{high}_{A,inst} - R\,.\,\tilde{\phi}^{low}_{A,inst} \neq 0$$

Notice that while antenna and source coordinates errors, given the non-dispersive nature of geometric terms, cancel out in this calibration procedure, a frequency dependent source position shift $\bar{\theta}_A$ would remain, since:

$$\phi^{high}_{A,geo} - R\,.\,\tilde{\phi}^{low}_{A,geo} = 2\pi\,\vec{D_\lambda}\,.\,\vec{\theta_A}$$

where $\vec{D_\lambda}$ is the baseline vector, in units of the higher wavelengths, and $\vec{\theta_A}$ stands for the "core-shift".

An integer frequency ratio $R$ will keep the phase ambiguity term in the phase equations as an integer number of $2\pi$, and avoid phase connection problems. We strongly advice to use the observations at a given frequency (*low*) to calibrate the harmonic frequencies (*high*). For simplicity we will omit the $2\pi$ ambiguity term in the coming equations. When $n$ is zero $R$ does not need to be integer, see Rioja et al. (2005).
Replacing the relations above in equation (1), the expression for the "frequency transferred" residual phases for the observations of source $A$ at the higher frequency becomes:

$$\phi^{FPT}_A = \phi^{high}_{A,str} + 2\pi\,\vec{D_\lambda}\,.\,\vec{\theta}_A + (\tfrac{1}{R} - R)\,\tilde{\phi}^{low}_{A,ion} + (\phi^{high}_{A,inst} - R\,.\,\tilde{\phi}^{low}_{A,inst}) \qquad (2)$$

The rapid tropospheric fluctuations have been calibrated out, however longer timescale contaminating ionospheric and instrumental terms remain blended with the radio structure and astrometric "core-shift" signature, and prevent its direct extraction from the phases. Previous applications of the dual-frequency calibration method used an extra step of self-calibration to remove these, with the consequent loss of the frequency-dependent position of the source (the "core-shift") in the sky (as in Middelberg et al. 2005).

We propose a different scheme that removes the non-dispersive terms while preserving the astrometric information. It uses the procedure of interleaving fast-frequency switching observations of the program source $A$ with those of a calibrator which is nearby in angle, $B$, in a very similar fashion as it is done for conventional phase referencing.

The analysis of the $B$ dataset is done following the same procedure as for $A$, and arrive to an equivalent expression to equation (2) for the FPT-phases of $B$:

$$\phi_B^{FPT} = \phi_{B,str}^{high} + 2\pi\, \vec{D_\lambda}\,.\,\vec{\theta_B} + (\tfrac{1}{R} - R)\,\tilde{\phi}_{B,ion}^{low} + (\phi_{B,inst}^{high} - R\,.\,\tilde{\phi}_{B,inst}^{low}) \qquad (3)$$

A careful planning of the observations, namely alternating between two sources that lie within the same ionospheric isoplanatic patch (whose size is many degrees at mm-wavelengths) with a duty cycle that matches the shortest ionospheric/instrumental time-scales (several minutes at least), results in the remaining dispersive terms in equations (2) and (3) being close to equal. That is:

$$(\tfrac{1}{R} - R)\,\tilde{\phi}_{A,ion}^{low} \approx (\tfrac{1}{R} - R)\,\tilde{\phi}_{B,ion}^{low}$$
$$\phi_{A,inst}^{high} - R\,.\,\tilde{\phi}_{A,inst}^{low} \approx \phi_{B,inst}^{high} - R\,.\,\tilde{\phi}_{B,inst}^{low}$$

Under these conditions the FPT-phases of $B$ can be used to calibrate the $A$ dataset, as in "conventional phase referencing". That is, apply self-calibration techniques on the FPT-phases from the $B$ dataset (including removal of the structure contributions), and transfer the estimated antenna-based corrections for the calibration of the FPT-phases of $A$, after interpolation to the corresponding observing times, $\tilde{\phi}_{B,self-cal}^{FPT}$.
The resultant SOURCE/FREQUENCY-REFERENCED residual phases for the target source $A$, $\phi_A^{SFPR}$, are free of ionospheric/instrumental corruption while keeping the astrometric "core-shift" signature:

$$\phi_A^{SFPR} = \phi_A^{FPT} - \tilde{\phi}_{B,self-cal}^{FPT} = \phi_{A,str}^{high} + 2\pi\vec{D_\lambda}\,.\,(\vec{\theta_A} - \vec{\theta_B})$$

where $\phi_{A,str}^{high}$ stands for the radio structure contribution of source $A$ at the high frequency, and the terms $2\pi\,\bar{D}_\lambda\,.\,\bar{\theta}_A$ and $2\pi\,\bar{D}_\lambda\,.\,\bar{\theta}_B$ modulate each baseline with a $\sim 24$ hours period sinusoid whose amplitude depends on the "core-shifts" in $A$ and $B$, respectively - and is equivalent to the functional dependence on the source pair angular separation in "conventional phase referencing".

Finally, the calibrated SFPR-visibility phases from the target source $A$, $\phi_A^{SFPR}$, are inverted to yield a synthesis image of source $A$ at the *high*-band, where the offset from the center corresponds to a bona-fide astrometric measurement of the combined frequency dependent "core shifts" in sources $A$ and $B$ between the *low* and *high*-frequency bands.

We have summarised the contributions to the residual phases and how they are handled in our new strategy for carrying out astrometric SOURCE/FREQUENCY PHASE REFERENCED observations. Because of the large calibration overhead involved in SFPR this method is only recommended for mm-VLBI, where no other method would succeed. Previous efforts to exploit the astrometric application of multi-frequency techniques failed (even for mm-VLBI), because of what is believed to be the ionospheric contribution. Whilst improved phase stabilisation

was achieved, and the deepest ever detection of VLBI cores at 86-GHz were produced, astrometric results could not. Our improved method compensates the remaining ionospheric and instrumental contributions while preserving the astrometric signature in the calibrated visibilities, and, of course, also increases the coherence integration time of the observations at the higher frequency.

We have not yet addressed the errors introduced by the interpolation of the lower frequency phase to the times of the high frequency observations (i.e. $\phi^{low}$ to $\tilde{\phi}^{high}$), nor the constraints on the frequency switching duty cycle, both closely related to the coherence at the time of the observations. Using a typical value for the Allan standard deviation ($\sigma_{Allan}$) of atmospheric phase fluctuations equal to $10^{-13}$ over 100 seconds (Thompson, Moran, Swenson 2001) and the accumulated phase noise ($\Delta\phi_a = 2\pi\nu\sigma_{Allan}\Delta\mathrm{t}$) one can estimate the coherence time ($\Delta$t) for a one radian change in phase. This results in typical coherence times of about 70 and 40 seconds, at 22 and 43 GHz, respectively. The duty cycle for the frequency switching has to be less than this coherence time for the lower frequency, if the conditions are typical. However normally one would normally request 'better than typical' weather conditions for mm-VLBI which would improve these limits. The error due to the interpolation of the low frequency phases to the time of the high frequency observations can be estimated from the errors ($\sigma_{low,i}$ for scan $i$) before and after the high frequency scan multiplied by the frequency ratio ($R$). If the duty cycle equals the coherence time the low frequency observations before and after the high frequency scan are independent, but (assumed to be) smoothly varying. Therefore, taking the errors as equal for the bracketing observations, the error on the high frequency observation is given by $R\sigma_{low}$. If the duty cycle is much less than the coherence time the errors will be $R\sigma_{low}/\sqrt{2}$ (as the measurements are independent, but the observables are not) however this will involve inefficient use of time in switching the frequencies. If the duty cycle is greater than the coherence time the solutions can not be connected with a linear extrapolation and the calibration will fail.

One can then deduce the minimum SNR required in the low frequency scans to ensure that the estimated phase corrections for the high frequency observations are meaningful. Assuming that $\sigma_{low}$ is given by the rms thermal phase noise formula ($\sigma_{low} \sim 1/\mathrm{SNR}$) and setting an upper limit of $30^o$ for the high frequency phase correction estimates, ones imposes SNRs in the low frequency scans equal to 6 and 11, for observations at frequency pairs 22/43 GHz and 22/86GHz, respectively. Note also that if one was choosing between using 22- or 43-GHz as the calibrator for an 86-GHz target one needs to balance the halving of the frequency ratio against the approximate three times higher SEFD for 43-GHz observations.

As an aside, the Korean VLBI Network (KVN), the world's first dedicated mm-VLBI array, will be able to observe 4 bands simultaneously (22/43/86/129 GHz). This will remove the need for frequency switching, tripling the observing time in a typical implementation thereby increasing the SNR, and furthermore remove the need for interpolation hence reducing the accumulated errors.

# 3 Demonstrations of the Method and Results

On 18 February 2007 we carried out 7 hours of VLBA observations of two pairs of continuum sources (1308+326 & 1308+328 $14'$ apart, and 3C273 & 3C274 $10^o$ apart), using fast frequency switching between 43- and 86-GHz scans on each source, and slow antenna switching between the sources, for each pair. Each antenna recorded eight 16-MHz IF channels, using 2-bit Nyquist sampling, which resulted in a data rate of 512 Mbps. The total duration of the observations was divided in ∼1.5-hour long blocks allocated to alternate observations of the two source pairs.

The analysis was done mostly using AIPS. See Dodson & Rioja (2008) for more details on the tasks and considerations. Firstly we followed the general VLBI calibration procedures, using the scans on the primary calibrator (3C273), and applied it to the total duration of the observations. Next, for each pair, we applied self-calibration analysis procedures to the observations of the two sources at 43 GHz (the "lower" frequency), scaled the resulting phase terms by a factor of 2 (using an external perl script), and applied these to the same source's observations at 86 GHz (the "higher" frequency). Then, we ran self-calibration procedures on the strongest source of each pair, 1308+326 and 3C273, respectively, at 86 GHz. These solutions were then transferred for calibration to the observations of the other source's pair, 1308+328 and 3C274, respectively, at the higher frequency, which were finally imaged without further calibration. The result of the analysis is, for each pair, is a SFPR map which contains the brightness distribution of the target source at 86 GHz, and where the offset of the peak of flux from the centre is astrometrically significant, and corresponds to the combined relative "core-shift" between 43 and 86 GHz, of both sources.

An additional complication that we have not mentioned above is related to the source radio structure effects; this is relevant when the sources are extended, as it is the case for the 3C pair. For this case both the lower frequency FRING phase solutions and the CALIB solutions (based on the best hybrid image) were doubled and applied for the calibration of the higher frequency observation. For compact sources, as it is the case for the 1308+326/8 pair, the structure contribution is negligible.

Figure 1 shows the SFPR image of 1308+328, at 86 GHz. This map was made following the method described above, using the 43-GHz observations of the source and further corrections derived from 1308+326, $14'$ away. The flux recovery in our image, defined as the ratio between the brightness peaks in the SFPR-map to the hybrid map, is 60%. For comparison, the only "conventional phase referenced" map which has been done at 86-GHz (Porcas & Rioja 2002), on this same pair of sources, resulted in a flux recovery of only 20%. Previous multi frequency VLBI observations of this pair of sources (Rioja et al. 1996) are compatible with a zero "core-shift", as found in our analysis.

Figure 2 shows the SFPR image of 3C274 (M87) at 86 GHz. The larger angular separation between the sources in the 3C pair, $10^o$ apart, compared to the $14'$ for the 1308+32 pair, makes this case a more challenging test. Still,

the flux recovery in the SFPR image in Figure 2 is 60%. The peak of brightness does show an offset from the centre of the map equal to 70$\mu$sec. In the absence of any other observations to compare our results with, we note here that the predicted "core-shifts" for 3C273 is 65 $\mu$sec, and zero for 3C274 (Lobanov, 1998 for 3C273 and personal comms. for 3C274), so it is possible that we again have a correct solution. As the theoretical predictions are not, at best, an exact science, it would be wise instead to take the measured "core-shift" in the map as an order of magnitude estimate of the reliability of the method. That is, we give an upper bound of 0.1 milli-arcsec to the astrometric accuracy produced by this strategy, pending further investigation.

# 4 Robustness of the Method vs. Weather

This method has also been shown to work well, in terms of astrometric recovery, in observations made without weather constraints. We summarize here the results found from the analysis of a series of 1-hour long VLBA test observations (Exp. codes BD123A/B/C) of the pair of sources 1308+326/8, with the VLBA, at 43 and 86 GHz. We followed the procedure described in section 3 for the analysis of the observations to produce SFPRed maps of 1308+328 at 86GHz, and also applied self-calibration procedures to produce hybrid maps, using AIPS.
The datasets were inspected and some baselines were flagged out based on lack of detections of the calibrator source.
To assess the quality of the results in the three sessions we used the ratio of the brightness peak values in the SFPRed to the hybrid maps, which we refer to as "flux recovery" hereafter. Calibration errors, arising from imperfect phase compensations in the analysis using a reference source/frequency, are responsible for the decrease, and biased positional offsets, of the peak flux in the SFPRed map.

Figure 3 shows the SFPRed maps of 1308+328 at 86-GHz obtained from the analysis of these observations. The map corresponding to the analysis of BD123B (*center*) shows 88% "flux recovery" with good solutions for all antennae in the dataset; for BD123C (*right*) the flux recovery is 60% with failed solutions for the NL and LA antennae; and for BD123A (*left*) the flux recovery is only 23%, with failed solutions the LA and PT antennae. The low "flux recovery" in the map from BD123A rises doubts about the success of the technique in that case. However the location of the peak flux in the three maps, which carries the astrometric information, does not significantly shift from the centre, with differences in positions $< 20\,\mu$as.

The weather conditions are expected to have an impact on the quality of the SFPR analysis results, as happens in conventional phase referencing. It would be very useful to have a threshold criterion for successful SFPR with respect to the weather conditions, especially at the highest frequencies. We could not address this question in this series of three test experiments since the weather "predictions" were not kept after the observations. We could not find either any outstanding correlation between the ground meteorological data measured

during the observations, or $T_{sys}$ values, and the image quality for the three experiments. Instead, we have attempted to characterize the weather, a posteriori, with phase coherence measurements using the observations themselves. We have used a four minutes long scan on the calibrator source 3C273 at 43 GHz, after preliminary calibration using a 2-minutes solution interval in FRING, for the three experiments. For each experiment the scans were segmented at different intervals (from 10 sec to 150 sec long, with 10 sec steps) and averaged (in scalar and vector fashion) to determine the visibility amplitudes. Figure 4 shows baseline phase coherence plots for the three experiments: the amplitude ratio between the vector average and scalar average in y-axis, against integration time in x-axis, for all baselines to the reference antenna in each of the three experiments. The plots only include baselines successfully detected in each session, using different colours for each antenna (in baselines with the reference antenna); the MK antenna (pink) shows the poorest coherence and the lowest ($\sim 30$) evelations in all the 3 experiments.

These experiments are so short (1-hour long) that this sample serves as a good indication of the conditions through-out the experiment. The plot for BD123B (*centre*) shows the best performance - better than can be resolved in the 2 min data-span. The coherence is certainly more than several minutes at 43 GHz, and corresponds to the session with best image recovery. For BD123C (*right*) the plot shows that severe coherence losses occur quite quickly, but then they reach a plateau and stabilize. The flux recovery in the map is 60%. Therefore we can say that the 2-minute solution interval is acceptable in this case. In experiment BD123A, the coherence shows a steady decrease across the span of the data. This is in agreement with the poor flux recovery, of only 23%, which would normally be described as a failure in the phase referencing process, although we repeat that the position of the peak of emission in the map is in agreement, to within 20 $\mu$as, with those from B and C datasets.

Based on Figures 3 & 4, a tentative classification of the weather conditions during the three 1-hour long observations, is: "good" for BD123B, "acceptable" for BD123B and "bad" for BD123A. The coherence times probe the weather conditions relevant for mm-wavelength observations, such as the content of water vapor in the troposphere, unobtainable from ground only meteorological measurements. We conclude that a suitable frequency duty cycle for obtaining a good SFPR map should be selected based on the observed frequencies and particular weather conditions during the observations; certainly it should be well under the coherence time at the reference (lower) frequency at the epoch of the observations. We are unable to give further guidance without further observations.

# 5 Summary

We have proposed and demonstrated a new method of astrometric VLBI calibration, suitable for mm-VLBI. It uses dual frequency observations to removed non-dispersive contributions. The additional step required to remove the iono-

spheric, and all other slowly varying dispersive terms, is done by including another source to cross calibrate with. Because the ionospheric patch size is very large at mm wavelengths one can use calibrators that lie a considerable distance from the source. We have presented the results from two pairs of sources, one only $14'$ apart and the other $10^o$ apart. A single pair is sufficient to demonstrate the method, however the astrometric solution (the offset from expected position) contains the contribution from both sources (as happens in standard phase-referencing as well). This problem, however, fulfills the closure condition, so three or more sources can be used to form a closure triangle and separate the contributions from each individual source.

## Acknowledgments

We wish to express our gratitude to Craig Walker, Ed Fomalont, Asaki Yoshiharu and Richard Porcas for their help in the development of the technique and in proof-reading this manuscript.

## References

[1] Asaki, Y., et al. 1998. "Phase Compensation experiments with the paired antennas method 2. Millimeter-wave fringe correction using centimeter-wave reference." Radio Science 33, 1297-1318.

[2] Carilli, C. L., Holdaway, M. A. 1999. "Tropospheric phase calibration in millimeter interferometry." Radio Science 34, 817-840.

[3] Dodson, R.. Rioja, M., 2008, "On the astrometric calibration of mm-VLBI using dual frequency observations", IT-OAN-2008-3

[4] Lobanov, A. P. 1998. "Ultracompact jets in active galactic nuclei." Astronomy and Astrophysics 330, 79-89.

[5] Middelberg, E., Roy, A. L., Walker, R. C., Falcke, H. 2005. "VLBI observations of weak sources using fast frequency switching." Astronomy and Astrophysics 433, 897-909.

[6] Porcas, R. W., Rioja, M. J. 2002. "VLBI phase-reference investigations at 86 GHz." Proceedings of the 6th EVN Symposium 65.

[7] Rioja, M. J., Dodson, R., Porcas, R. W., Suda, H., Colomer, F. 2005. "Measurement of core-shifts with astrometric multi-frequency calibration." ArXiv Astrophysics e-prints arXiv:astro-ph/0505475.

[8] Rioja, M. J., Porcas, R., Machalski. J. 1996. "EVN Phase-Referenced Observations of 1308+328 and 1308+326." Extragalactic Radio Sources, IAU Symp. 175, p. 122.

[9] Thompson, Moran, Swenson, 2001, "Interferometry and Sythesis in Radio Astronomy" (New York: John Wiley & Sons)

**Acknowledgments** we wish to note the essential help of the EU Marie-Curie International Incoming Fellowship (MIF1-CT-2005-021873), the VLBA which in funded by the National Science Foundation (of the USA) and the support of and advice from Ed Fomalont, Richard Porcas and Vivek Dhawan.

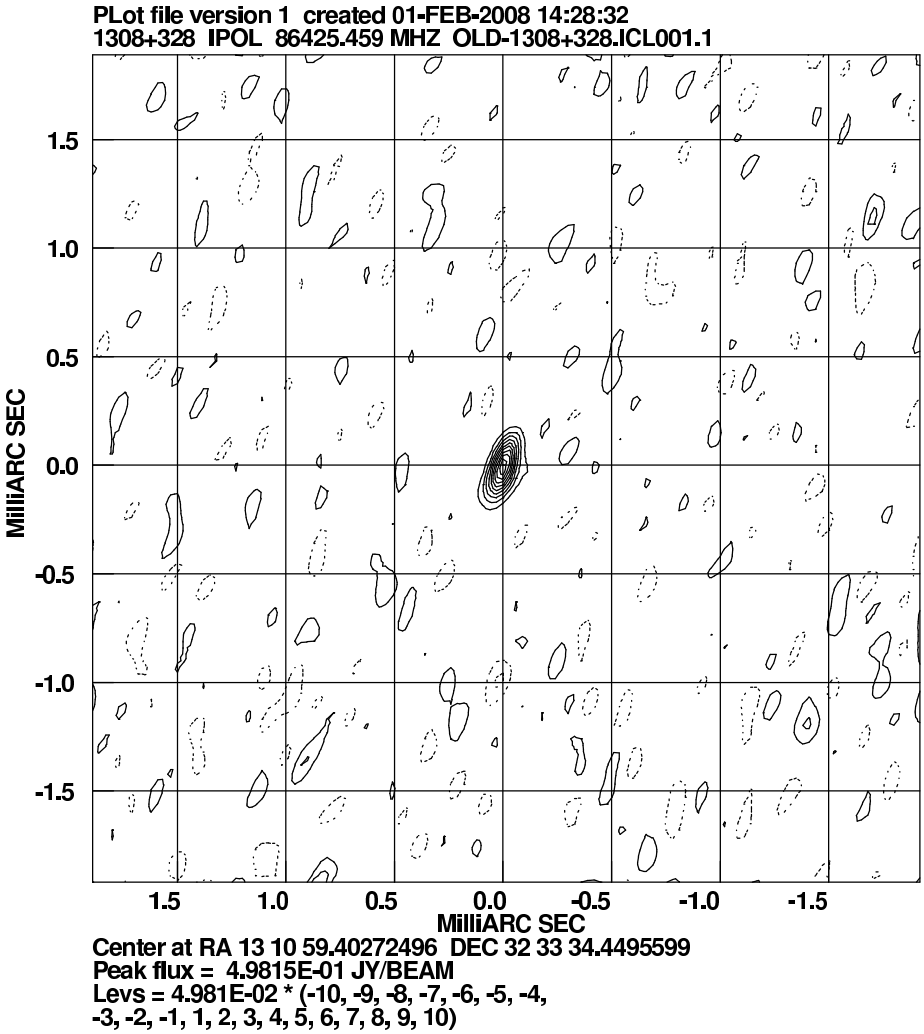


Figure 1: SFPR map of 1308+328, at 86 GHz, calibrated with the 43 GHz phases and further corrections from 1308+326 – 14′ away. The offset from the phase centre is zero to within the errors, as expected from other phase-referencing experiments. The flux recovery compared to the hybrid map is 60%.

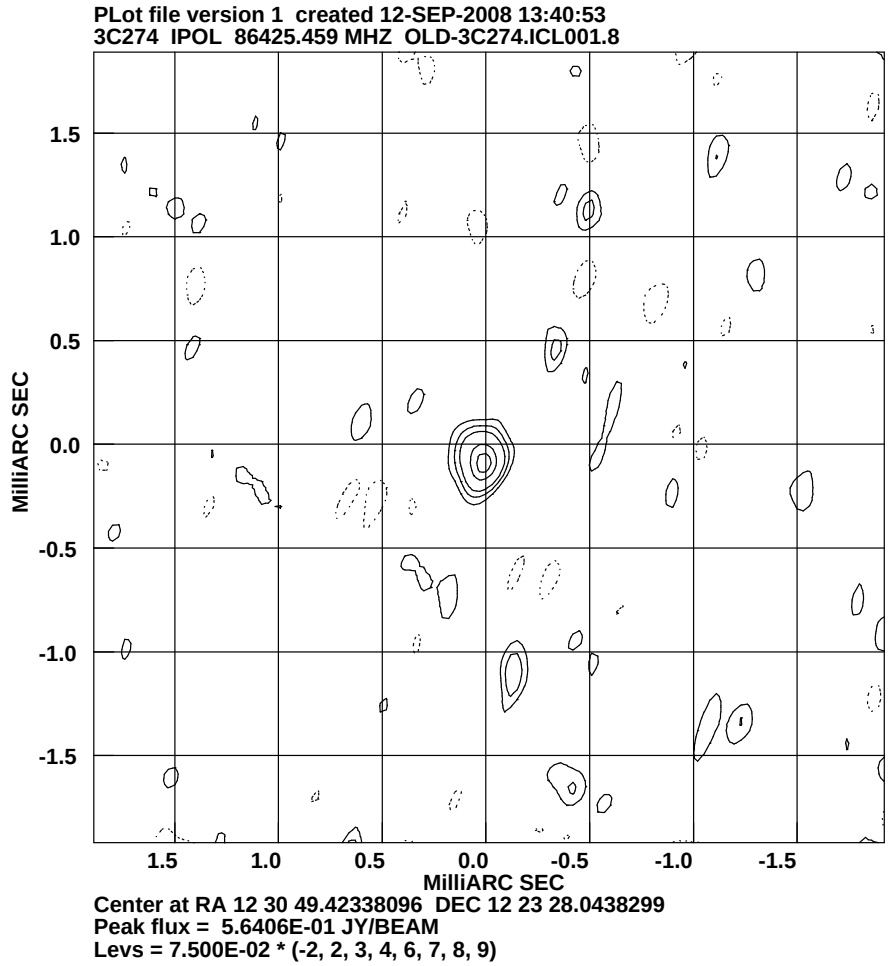


Figure 2: SFPR map of 3C274, at 86 GHz, calibrated with the 43 GHz phases and further corrections from 3C273 – $10^o$ away. The offset from the phase centre (70 $\mu$sec) is close to that predicted on theoretical grounds. The flux recovery compared to the hybrid map is 60%.

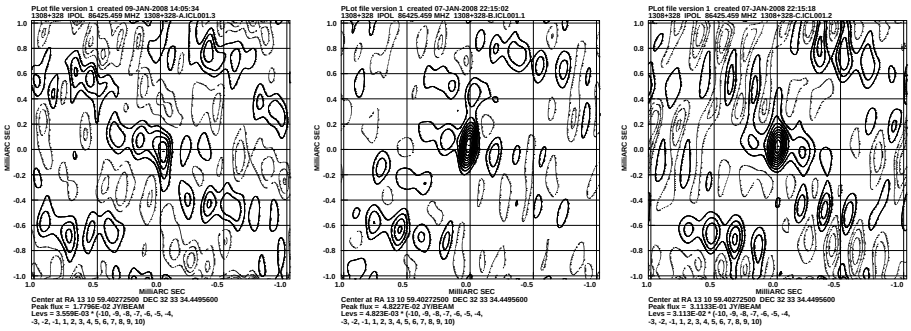

Figure 3: Montage of SFPR maps of 1308+328, at 86 GHz, from our 1-hour long VLBA observations. The flux recovery compared to hybrid maps is 88% for BD123B (centre), 60% for BD123C (right) and 23% for BD123A (left). All experiments produce comparable astrometric results, to 20$\mu$arcsec.

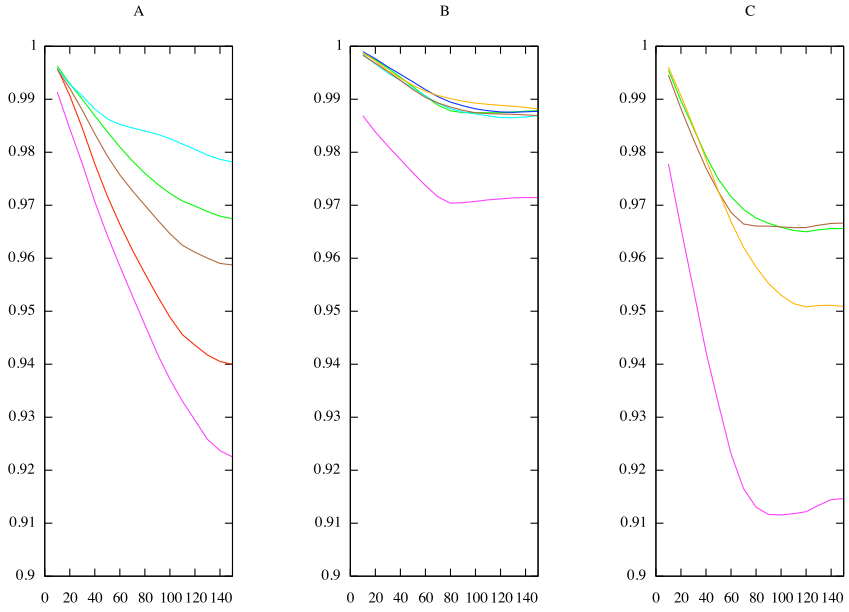


Figure 4: Coherence of the data for each of the three epochs of BD123. Plotted is coherence (vector average over scalar) against time in seconds on the primary calibrator 3C273. The different antennae are plotted in different colours. The best weather (B, centre) produces the best flux recovery (88%), the worst results (23%) come from the worst weather (A, left), however the weather for the third epoch (C,right) is not much better however the flux recovered is 60%.